



Research Article/Araştırma Makalesi

Dynamic effects of piezoelectric fan on the natural convection in a vertical channel

Özgün Alkım Boz¹, Serhan Küçüka², Mehmet Akif Ezan^{1,2,3}

¹Dokuz Eylül University, The Graduate School of Natural and Applied Sciences, Buca, Izmir, Türkiye

²Dokuz Eylül University, Faculty of Engineering, Department of Mechanical Engineering, Buca, Izmir, Türkiye

³Dokuz Eylül University, Energy Application and Research Center (EUAM), Buca, Izmir, Türkiye

Keywords

Piezoelectric fan
Oscillating fan
Natural convection
Vortex generation

Article history:

Received: 27.03.2024

Accepted: 09.05.2024

Abstract: In this study, the dynamic heat transfer characteristics of a piezoelectric fan (piezo fan) placed in a vertical channel with constant temperature side walls were investigated numerically. One of the piezo fan's ends is fixed like a cantilever fan, and the other end performs oscillation motion at four different amplitudes and three different frequencies. The operating amplitude of the fan has been varied in such a way as to investigate the temperature distributions, pressure variations, and dynamic mechanisms of the vortices inside the channel. Numerical studies were carried out using a 2-dimensional model in the COMSOL Multiphysics software. Pure natural convection inside the channel is considered as a reference case. The piezo fan's movement creates high-speed vortices along the flow direction, pushing them onto wall surfaces. Such complex convective mechanisms positively affect heat transfer through the hot wall. Each case's local and average heat transfer coefficients and Nusselt numbers are compared. As a result, the piezoelectric fan operating with 12 mm amplitude and 20 Hz frequency was determined to be the most effective design with a heat transfer improvement of 169% compared to the natural convection. For the highest amplitude and frequency, the increment in the mass flow rate is up to 180%.

To Cite/Atıf için:

Boz Ö.A. Küçüka S., Ezan M.A. Dynamic effects of piezoelectric fan on the natural convection in a vertical channel. International Journal of Technological Sciences, 16(1), 1-10, 2024.

Düşey kanalda piezoelektrik fanın doğal taşınım üzerindeki dinamik etkileri

Anahtar Kelimeler

Piezoelektrik fan
Salınımlı fan
Doğal taşınım
Girdap oluşumu

Makale geçmişi:

Geliş Tarihi: 27.03.2024

Kabul Tarihi: 09.05.2024

Öz: Bu çalışmada yanal duvarları sabit sıcaklıkta tutulan düşey bir kanal içerisine yerleştirilen piezoelektrik fanın (piezo fan) dinamik ısı transfer karakteristikleri sayısal olarak incelenmiştir. Piezofanın bir ucu konsol fan gibi sabitlenmiş olup, diğer ucu dört farklı genlik ve üç farklı frekansta salınım hareketi gerçekleştirmektedir. Kanal içindeki sıcaklık dağılımları, basınç değişimleri ve girdapların dinamik mekanizmaları araştırılacak şekilde fanın genliği farklılaştırılmıştır. Sayısal çalışmalar COMSOL Multiphysics yazılımında 2 boyutlu model kullanılarak gerçekleştirilmiştir. Kanal içerisindeki doğal taşınım referans durum olarak ele alınmıştır. Piezo fanın hareketi, akış yönü boyunca yüksek hızda girdaplar oluşturarak bunları duvar yüzeylerine itmektir. Bu tür karmaşık taşınım mekanizmaları ısıtılan duvardan gerçekleşen ısı transferini olumlu yönde etkilemektedir. Ele alınan tüm durumlar için yerel ve ortalama ısı transfer katsayıları ve Nusselt sayıları karşılaştırmalı olarak sunulmuştur. Sonuç olarak 12 mm genlik ve 20 Hz frekansta çalışan piezoelektrik fanın, doğal taşınımına göre %169 ısı transfer iyileştirmesi ile en etkili tasarım olduğu belirlenmiştir. En yüksek genlik ve frekans için kütleli debideki artış ise %180 olarak elde edilmiştir.

1. Introduction

One of the methods to increase the heat transfer from a hot surface is placing a piezo fan in front of the heated wall, as piezo fan oscillation creates vortices and

enhances the convective heat transfer. Piezoelectric fans have a flexible blade supported at one end and a piezoelectric part attached. Applying electrical current to the piezo part vibrates the blade at the resonant frequency. This vibration causes high-amplitude

oscillations at the free end so that the fan creates vortices on both sides of the blade that rotate in opposite directions [1]. The vortices rotating in the opposite direction cause the downstream free flow velocity to increase. The distance between the vortices increases when the free flow velocity increases. The two critical parameters affecting the heat transfer are the amplitude and frequency of the piezo fan. The flow rate of the air is proportional to the width and thickness of the piezoelectric fan, but it is not affected by its length [2].

In the literature, piezo fans are mostly located in the channel flow to improve the heat transfer rate. Wait et al. [3] studied the airflow induced by the piezo fan oscillations. They studied with two different resonance values. It is obtained that operating the piezo fan at high frequencies reduces efficiency while increasing energy consumption. The effect of piezo fan length on the flow field is also investigated in the same study. The transient and steady-state fluid motion around the fan blade is presented in detail. Operating in high resonance modes increases power consumption and decreases airflow. Lin [4] experimentally and numerically investigated the effect of the flow field around a piezo fan on heat transfer. The piezo fan was positioned vertically and horizontally on the heated surface. On both sides of the oscillating blade, oppositely moving and screw-like streamlines were observed. When the fan is placed vertically on the heated surface, improvement in heat transfer is observed to be between 60% and 240%. The enhancement is between 80% and 260% for horizontally located fans. Lin [5] used a cylindrical surface and placed eighteen thermocouples to measure the temperature variation across the surface. As a result, the piezo fan increased the heat transfer coefficient at different points by 20% to 240%, and the average surface temperature decreased by 20°C. Park et al. [6] conducted a 3-dimensional simulation of the oscillating movements of a piezo fan placed in the middle of a channel with airflow. The piezoelectric fan adversely affects the axial flow rate and slows the fluid at high speeds. In contrast, the piezoelectric fan increases the flow rate in the axial direction at low speeds. Tiwari and Yeom [7] operated the piezoelectric fan at a frequency of 90.3 Hz and an amplitude of 11.8 mm. The heat transfer in a horizontal channel of 22.5 mm × 22.5 mm is investigated experimentally and numerically. The heated surface is 22 mm wide and 52 mm long and is placed on the channel floor in front of the piezo fan. A piezoelectric fan made from nickel and the flexible blade material Bi-Morph with a length of 20 mm is used in the channel. Numerical studies were carried out using the ANSYS Fluent software. It has been found that the form of vortex structures is the key factor affecting the heat transfer rate of the hot surface in the channel.

The highest heat transfer enhancement, 102%, is obtained when the piezo fan is placed in front of the heated surface. Chen et al. (2020) [8] studied the effect of a piezoelectric fan on heat transfer inside a horizontal channel. Uniform heat flux is defined on the channel surface. Firstly, the piezoelectric fan frequency was selected as 43 Hz, and Reynolds numbers of 8500, 13700, and 19100 were tested. The highest heat transfer rate was achieved at the Reynolds number of 19100. As a second step, at $Re = 19100$, the frequencies of 43 Hz, 35 Hz, and 0 Hz were examined to determine the influence of frequency. The highest heat transfer rate was observed in the case of the piezo fan operating with a 43 Hz frequency. In recent studies, Hasan et al. [8]-[9] numerically studied the effect of piezo fans on heat transfer in horizontal and vertical channels. Hasan et al. [8] placed a piezoelectric fan on a hot surface with a laminar flow inside a horizontal air channel. Maximum heat transfer enhancement was obtained to be 231%. Hasan et al. [9] investigated the effect of a piezo fan in the middle of a vertical channel. It was stated that there were improvements of up to 127% in heat transfer when the piezo fan was used in a channel with natural convection. However, in the case of forced convection, the piezo fan limits the increase in heat transfer by dragging the vortices.

Under appropriate design and working conditions, Piezo fans induce more enhanced heat transfer than natural convection. A significant increase in heat transfer coefficients can be achieved depending on the amplitude and frequency of the piezo fan. This study investigates the effects of piezo fans in the vertical channel on heat transfer in different operating situations, along with the effects of natural convection. Numerous studies exist on the impact of various positions of the piezo fan relative to the heated surface. In this study, numerical analysis of the piezo fan placed in the vertical direction on the channel axis was performed at different frequencies and amplitudes, and the variation of the heat transfer depending on the amplitude and frequency was investigated. As a novelty, the current study considers both the vortex structures, local and average heat transfer characteristics and proposes a Nusselt correlations in terms of the dimensionless Reynolds number defined regarding the tip speed of the blade.

2. Materials & Method

This section defines the problem with related initial and boundary conditions, and then the solution methodology and validation are represented.

2.1. Definition of the Problem

The 2D mathematical model with geometrical dimensions and thermal boundary conditions is given in Figure 1. Near the vertical channel's entrance is a piezo fan at the symmetry line. The fan is fixed at the lower end and vibrating symmetrically on the upper side. The side walls from the upper end of the fan through the outlet of the channel are kept at constant temperatures of 80°C. The incompressible laminar flow model with the Boussinesq approach was used to analyze mixed flow in the channel. Gravity is defined along the negative y -direction. The walls from the channel's entrance to the heated side walls are adiabatic. The inlet temperature of the fluid is 20°C. The solid mechanics module, including the moving boundary condition, is selected for the piezo fan. Transient analyses are conducted to monitor the piezo fan oscillations, and analyses proceed until reaching a cyclic regime in the thermal characteristics.

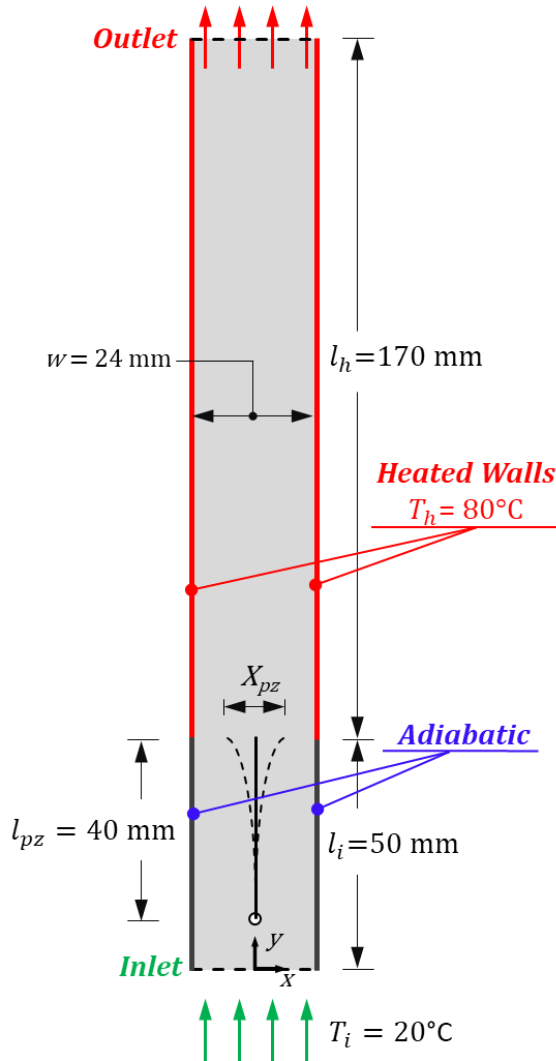


Figure 1. 2D channel geometry with piezo fan

2.2. Governing Equations with Initial and Boundary Conditions

The COMSOL Multiphysics software resolves the coupled fluid/solid interactions. The following governing equations are considered to evaluate the transient heat transfer inside the computational domain:

Continuity equation:

$$\frac{\partial u}{\partial x} + \frac{\partial v}{\partial y} = 0 \quad (1)$$

Momentum equations:

x -direction:

$$\rho \frac{\partial u}{\partial t} + \rho u \frac{\partial u}{\partial x} + \rho v \frac{\partial u}{\partial y} = -\frac{\partial p}{\partial x} + \mu \frac{\partial^2 u}{\partial x^2} + \mu \frac{\partial^2 u}{\partial y^2} \quad (2)$$

y -direction:

$$\rho \frac{\partial v}{\partial t} + \rho u \frac{\partial v}{\partial x} + \rho v \frac{\partial v}{\partial y} = -\frac{\partial p}{\partial y} + \mu \frac{\partial^2 v}{\partial x^2} + \mu \frac{\partial^2 v}{\partial y^2} - (\rho - \rho_{ref})g \quad (3)$$

Energy equation:

$$\rho c_p \frac{\partial T}{\partial t} + \rho c_p u \frac{\partial T}{\partial x} + \rho c_p v \frac{\partial T}{\partial y} = k \frac{\partial^2 T}{\partial x^2} + k \frac{\partial^2 T}{\partial y^2} \quad (4)$$

The inlet is defined as an open boundary condition. According to this, atmospheric pressure is defined at the inlet with a normal stress (f_o) value of zero. The inlet temperature is the same as the surrounding temperature of air:

$$@y = 0 : P_i = P_{atm}, \quad f_o = 0, \quad T_i = 20^\circ\text{C}$$

At the outlet section, the pressure is equal to atmospheric pressure,

$$@y = l_i + l_h : P_o = P_{atm}$$

The no-slip boundary condition is defined for velocity on the channel walls. The walls are adiabatic up to the end of the piezo fan at the entrance, and then a constant temperature of 80°C is defined,

$$@x = \pm w/2, \quad 0 \leq y \leq l_i + l_h : u = v = 0$$

$$@x = \pm w/2, \quad 0 \leq y \leq l_i : \partial T / \partial x = 0$$

$$@x = \pm w/2, \quad l_i \leq y \leq l_i + l_h : T = T_h$$

A reference temperature is defined for the calculation of the buoyancy force. The initial temperature of the air in the channel is equal to the reference temperature,

$$T_{ref} = 20^\circ\text{C}, T_{int} = T_{ref}$$

2.3. Equations for Fan Displacement

The blade's displacement during the piezo fan oscillation depends on the fan material and geometric

properties. The displacement function used for a rectangular and fixed cross-section cantilever fan is given as [11]:

$$X_{pz}(y) = \psi A_{pz} \left\{ [\sin(\beta_{pz} l_{pz}) - \sinh(\beta_{pz} l_{pz})] [\sin(\beta_{pz} y_{pz}) - \sinh(\beta_{pz} y_{pz})] + [\cos(\beta_{pz} l_{pz}) - \cosh(\beta_{pz} l_{pz})] [\cos(\beta_{pz} y_{pz}) - \cosh(\beta_{pz} y_{pz})] \right\} \quad (5)$$

where l_{pz} represents the length of the piezo fan and A_c represents the cross-sectional area. ψ is the dimensionless drive coefficient related to the driving intensity applied to the piezo fan blade from the outside. It can be set by changing the electrical voltage intensity applied to the piezo fan material. β_{pz} is a characteristic coefficient dependent on material properties as [9]:

$$\beta_{pz} = \sqrt[4]{\frac{2\pi f m_{pz}}{l_{pz}^4 E_{pz}}} \quad (6)$$

The displacement of the piezo fan blade with respect to time varies depending on the applied electrical voltage. For sinusoidal voltage variation, the harmonic displacement of each point is given as [9]:

$$x_{pz}(y, t) = X_{pz}(y) \sin(2\pi f t) \quad (7)$$

The velocity variation of each point by taking its derivative in time as [9]:

$$u_{pz}(y, t) = X_{pz}(y) 2\pi f \cos(2\pi f t) \quad (8)$$

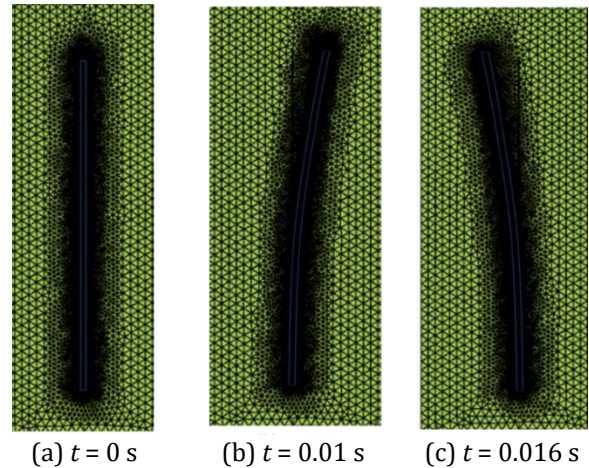
2.4. Mesh Structure

The equations described above were analyzed using the finite element method with the COMSOL Multiphysics software. The interaction between the moving fan surface and the surrounding fluid (*air*) is defined using the Fluid Structural Interaction (FSI) module. The geometry of the fan distorts depending on the oscillation, so the mesh structure is re-formed at each time step. The ALE method solves the flow in the mesh structure that changes shape over time. The mesh structure around the fan blade at the beginning of the movement is shown in Figure 2. The mesh intensity is much tighter adjacent to the piezoelectric fan since the meshes are compressed and deformed in the direction of movement.

Preliminary analyses are conducted to observe the influence of mesh structure and time step size on the mass and energy conservation of the model. The time step was taken in the literature at different values between 1/40 and 1/400 of the period [11,12]. In the current study, the initial time step was taken as 0.001 s, corresponding to 1/100 of a period for a frequency of 10 Hz and 1/50 for a period for a 20 Hz frequency. The

software adaptively modifies the time step size. As the progress proceeds and the convergence improves, the program dynamically increases the time step size to complete the simulation faster.

Numerical results were obtained for three different mesh structures, with 13692 for the coarse condition, 21816 for the normal, and 29710 for the fine mesh structure. In the sample case studied, the piezo fan in the channel oscillates with an amplitude of 15 Hz and 12 mm. Initially, the air in the channel is at a temperature of 20°C and is stagnant. The variation of the average fluid temperature at the channel outlet in time is given in Figure 3. The outlet temperature is initially equal to the initial temperature (20°C). After an irregular transition period, the outlet temperature settles towards a stable value with narrow fluctuations. The variations in outlet temperature have similar characteristics for the three mesh structures, yet it is clear that coarse mesh is insufficient to capture the process accurately. The normal and fine mesh structures, on the other hand, overlap. As the heavy mesh structure causes computational difficulties and extends the simulation time, the normal mesh structure is selected for the rest of the simulations.



(a) $t = 0$ s (b) $t = 0.01$ s (c) $t = 0.016$ s
 Figure 2. The mesh structure around the piezo fan and its deformation with the movement of the blade ($f = 15$ Hz $2A = 12$ mm)

2.5. Validation

The validity of the developed mode is tested by considering the numerical and experimental studies of Acikalin and Garimella [13]. Figure 4 shows the geometry and boundary conditions of the validation study. 650 W/m² of uniform heat flux is defined on the hot surface, and the piezo fan oscillates at 62.5 Hz and 10 mm amplitude in the middle of the hot surface. The local heat transfer coefficient variation on the hot wall is compared against the experimental and numerical results from the literature. Figure 5 compares the

current predictions against the results taken from the literature. The results of the numerical studies are similar to those of other studies, and a maximum discrepancy of $\pm 11.5 \text{ W/m}^2\text{K}$ is obtained compared to the experimental study.

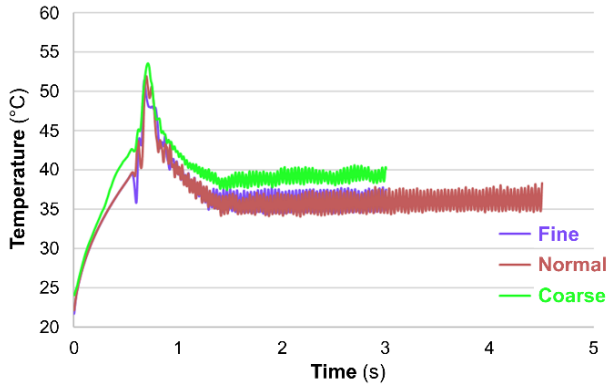


Figure 3. Effect of mesh structure on the variation of average fluid outlet temperature with time

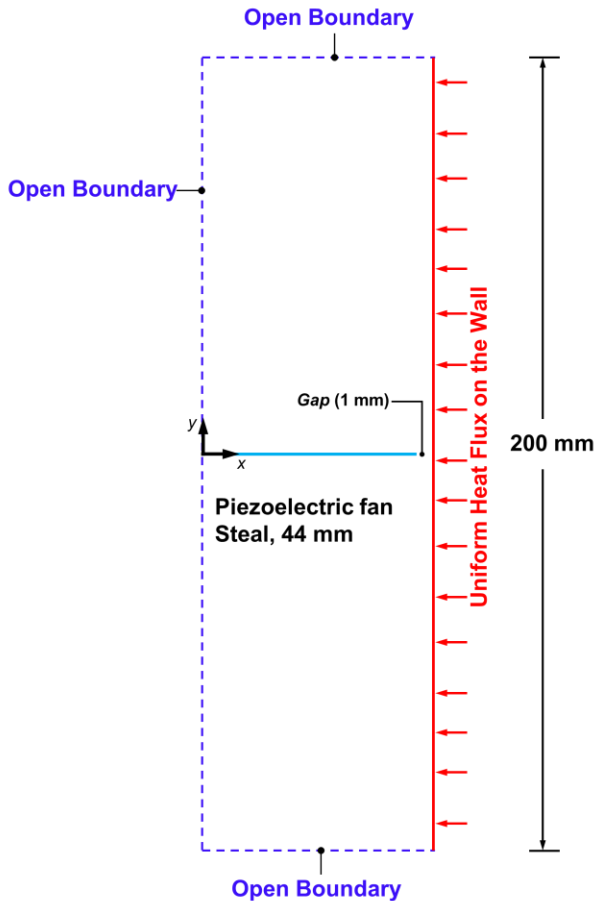


Figure 4. The geometry and boundary conditions of the validation study [13,14]

2.6. Data Reduction

The local heat transfer coefficient on the heated walls of the channel is defined in terms of the heat flux and the temperature difference as

$$h = \frac{q''}{(T_h - T_i)} \quad (9)$$

In order to evaluate the oscillation effect, the average speed of the piezo fan tip is taken into account. Accordingly, the Reynolds number is defined as

$$Re_{tip} = \frac{u_{tip} W}{\nu} \quad (10)$$

The Strouhal number is defined in terms of the frequency and the mean velocity at the channel section as

$$St = \frac{f 2A}{U_{mean}} \quad (11)$$

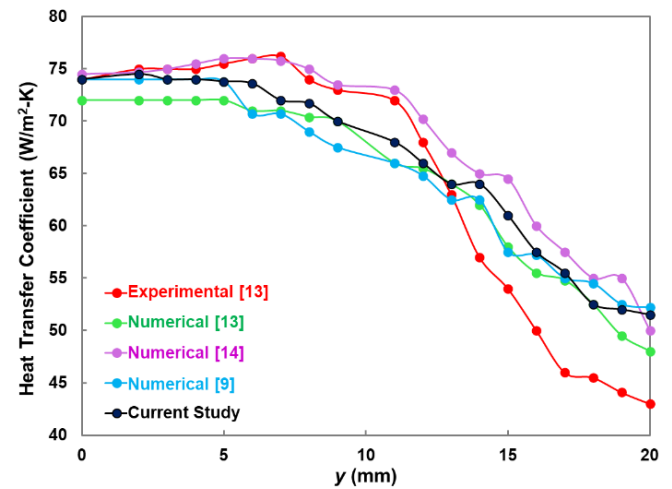


Figure 5. Comparison of predicted results with the literature [10,13,14]

The Nusselt number defines the dimensionless heat transfer on the channel wall as

$$\overline{Nu} = \frac{\bar{h} w}{k} \quad (12)$$

where \bar{h} is the average heat transfer coefficient on the heated wall and is evaluated from local variations of the heat transfer coefficient as defined in Eq. (9).

3. Results & Discussions

In this section, numerical mass flow and heat transfer results are obtained by operating the piezo fan at different amplitudes and frequencies. The effect of piezo fan oscillation on flow and heat transfer is

parametrically investigated. Depending on the material and the geometry of the blade, the piezo fan frequency is defined to be 5 Hz, 10 Hz, and 20 Hz. On the other hand, the blade's amplitude varies from $2A = 6$ mm to $2A = 12$ mm. The mesh intensity should be denser at higher amplitudes to accurately compute the pressure and velocity variations around the blade. Such an attempt not only exponentially increases the time for numerical simulations but also adversely affects the convergence of the simulation and significantly reduces the accuracy of the predicted results. Considering the mentioned limitations, the amplitude is limited to $2A = 12$ mm. Including the pure natural convection case (NC), a total of 13 cases are studied. For each case, the simulations proceed until the cyclic steady state is obtained. The transient and steady vortex structures are discussed in detail in the first sub-section. The parametric thermal and hydrodynamic results, including the local variations, are given in the second sub-section. The time for the total internal energy in the channel to reach an approximately constant value is taken as the steady state time.

3.1. Vortex Structures inside the Channel

Figure 6 represents the evolution of the velocity field and vortices for $f = 20$ Hz and $2A = 12$ mm. For a piezo fan oscillating with a frequency of $f = 20$ Hz, the cycle time is 0.05 s; that is, four instances of $t_1 = 0.0078$ s, $t_2 = 0.0249$ s, $t_3 = 0.0332$ s and $t_4 = 0.0506$ s are selected to provide a complete understanding of the tip vortex behavior of the blade while moving to the right and left. Notice that the red arrows in Figure 6(a) represent the direction of the blade movement. It is observed that while the blade is moving to the right, a tip vortex with a counterclockwise direction is developed at the rear of the blade. On the contrary, a clockwise vortex is developed while the blade moves to the left. The oscillating piezo fan continuously develops counter-current vortices on the blade's tip. With the effect of local forces and natural convection, they move towards the channel outlet along the y -direction.

The movement of the vortices along the upward direction inside the channel is shown in Figure 7 at $t = 2$ s, for the same frequency and amplitude as in Figure 6, i.e., $f = 20$ Hz and $2A = 12$ mm. The vortices form at the tip of the piezo fan and move towards the outlet of the channel in the positive y -direction. The highest velocity is observed at the tip of the piezo fan, and the velocity magnitude reduces towards the outlet.

Figure 8 shows the vortex shedding developed by the oscillated piezo fan along the channel throughout a period of the piezo fan motion. Here, the results are provided from $t = 2$ to $t = 2.05$ s. One should infer that

the strong vortices adjacent to the blade tip weaken towards the channel outlet.

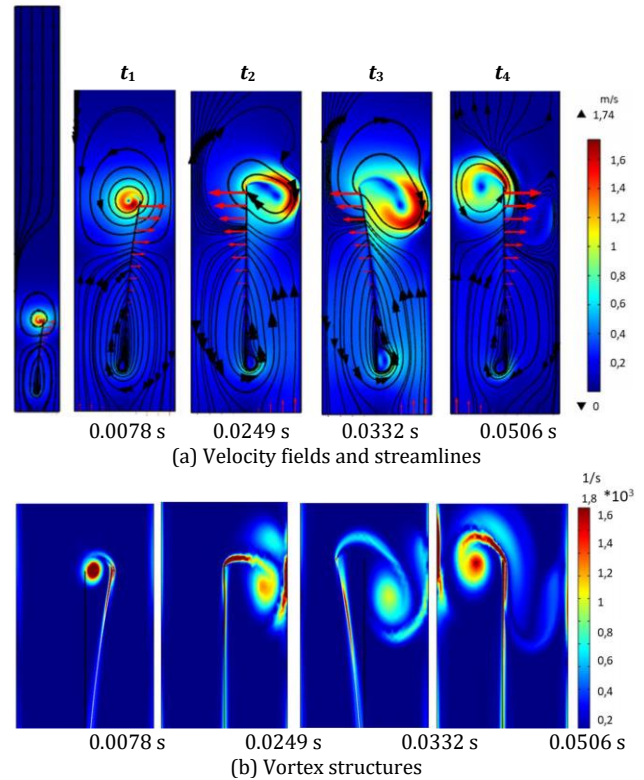


Figure 6. Evolution of velocity fields and vortex structures around the piezo fan in the first period for $f = 20$ Hz and $2A = 12$ mm

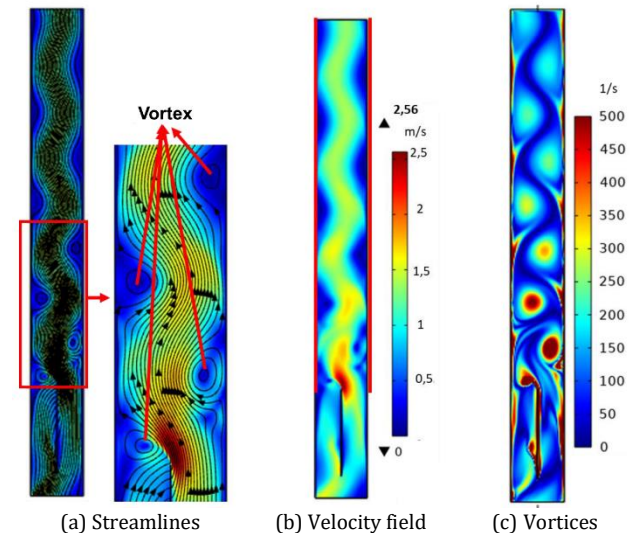


Figure 7. Vortex structures inside the channel at $t = 2$ s for $f = 20$ Hz and $2A = 12$ mm

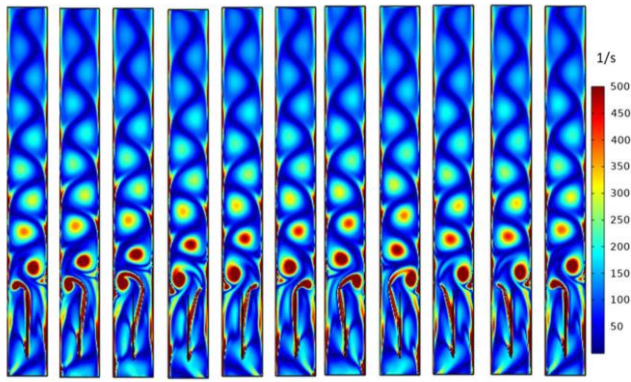


Figure 8. Evolution of the vortex structures in a periodic of the piezo fan ($f = 20$ Hz and $2A = 12$ mm)

Figure 9 shows the pressure variations around the piezo fan during the first period of oscillation. Arrows indicate the direction of the blade motion. The blade pushes the air through left and right at $t = 1.982$ s and $t = 2$ s, respectively. It is observed that pressure increases in the direction of the movement, and at the rear side of the blade, there is a low-pressure region. Vortex develops due to the low pressure at the rear side, and pressure difference plays a key role in the formation and growth of vortices.

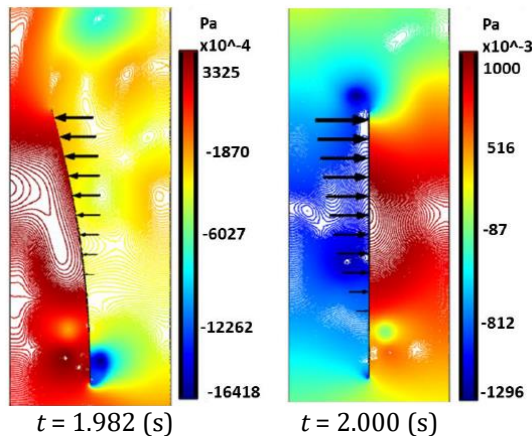


Figure 9. Evolution of the vortex structures in a periodic of the piezo fan ($f = 20$ Hz and $2A = 12$ mm)

3.2. Parametric Results

A total of 13 simulations were conducted in the current study. The selected parameters and main outputs of the simulations are listed in Table 1. For each case, the fan tip velocity, air mass flow rate per unit depth, the mean outlet velocity, the heat transfer per unit depth, and the average outlet temperature at the outlet section are evaluated. Notice that the tip velocity of the piezo fan and the mass flow rate of air significantly improve as the frequency and amplitude of the piezo fan increase. Increased convection enhances the extracted heat from the heated surfaces, and using a piezo fan increases the heat transfer. In the natural convection case, the heat

transfer rate is 144.9 W/m. For instance, for a piezo fan with a frequency of 20 Hz and an amplitude of 12 mm, the heat transfer rate reaches 389.6 W/m with an increase of 169% compared to the natural convection case. In this sub-section, some local variations are provided to discuss the influence of piezo fan motion on the heat transfer characteristics.

Table 1. Variation of mass flow, heat transfer rate, mean outlet velocity, and temperature of air for different frequencies and amplitudes

f (Hz)	$2A$ (mm)	u_{tip} (m/s)	\dot{m}' (kg/ms)	u_{outlet} (m/s)	q' (W/m)	T_{outlet} (°C)
NC	-	-	0.00982	0.3398	144.9	34.7
10	6	0.12	0.01038	0.3592	165.4	35.6
10	8	0.16	0.01202	0.4157	198.5	36.4
10	10	0.20	0.01337	0.4628	224.7	36.7
10	12	0.24	0.01465	0.5055	249.7	37
15	6	0.18	0.01131	0.3914	173.5	35.2
15	8	0.24	0.01363	0.4716	210.8	35.4
15	10	0.30	0.01805	0.6243	259.6	34.3
15	12	0.36	0.02108	0.7303	315	34.9
20	6	0.24	0.01275	0.4411	180.6	34
20	8	0.32	0.01584	0.5482	239.4	35
20	10	0.40	0.02219	0.7677	311.8	34
20	12	0.48	0.02775	0.9601	389.6	34

In Figure 10, the velocity and temperature variations at the outlet section of the channel are provided at $t = 2$ s. Piezo fan motion improves the maximum fluid velocity more than three times and slightly shifts the mean fluid temperature. The temperature distribution is given in Figure 10(c). One should notice that the piezo fan motion disturbs the boundary layer along the flow direction, and consequently, the temperature variation given in Figure 10(b) becomes flattened.

The variation of the heat convection coefficient along the channel surface is shown in Figure 11. At the point where the hot surface starts, the sudden temperature change in the boundary layer causes the heat transfer coefficient to reach the highest value. The heat transfer coefficient exponentially reduces due to the growing boundary layer in the pure natural convection case. Piezo fan motion, on the other hand, breaks the boundary layer development so that the heat transfer coefficient makes fluctuations along the channel height. Increasing the amplitude increases the fluctuations and shifts the variations. Along the flow direction, the heat transfer coefficient decreases due to the development of the boundary layer weakening the vortices.

Table 2 presents the effects of the piezo fan operated at different amplitudes and frequencies on the heat transfer coefficient and dimensionless numbers. Dimensionless Reynolds, Nusselt, and Strouhal numbers are provided to generalize the outputs. One may notice that the influence of amplitude becomes more apparent in higher oscillating frequencies. At 10 Hz, compared to the baseline case, i.e., NC, the maximum

increment in the Nusselt number is 72.3%, and the increment reaches 168.9% for the same amplitude at 20 Hz. One may presume that considerable power is required to drive the piezofan to achieve such enhancements in heat transfer. Yet the power consumption of the piezo fan is in the order of 1 mW/m for the current simulations. Wait et al. [15] and Kimber et al. [16] also reported the same order of power consumption for piezo fans with similar materials. Considering the enhancements in the heat transfer rates per unit depth of the channel summarized in Table 1, the piezo fan's power consumption could be considered negligible.

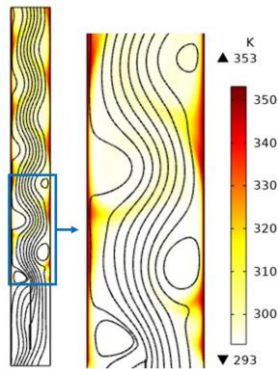
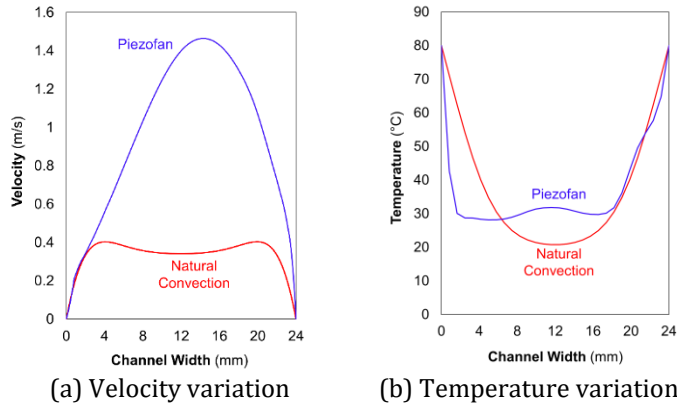


Fig. 10. Effect of the piezo fan on velocity and temperature variations along the channel width ($f = 20$ Hz, $2A = 12$ mm)

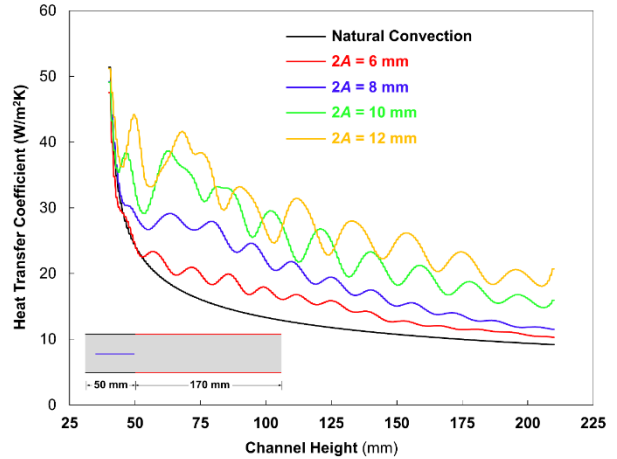


Figure 11. Variation of heat transfer coefficient along the channel height ($f = 15$ Hz, $t = 3$ s)

Table 2. Reduced results with nondimensional parameters

f (Hz)	2A (mm)	Re	\bar{h} (W/m ² K)	Nu	St	% Increment
NC	-	-	7.1	6.8	-	-
10	6	185.6	8.1	7.8	0.167	14.1
10	8	247.4	9.7	9.3	0.192	37.0
10	10	309.3	11.0	10.6	0.216	55.1
10	12	371.1	12.2	11.8	0.237	72.3
15	6	278.4	8.5	8.2	0.229	19.7
15	8	371.1	10.3	9.9	0.254	45.5
15	10	463.9	12.7	12.2	0.240	79.2
15	12	556.7	15.4	14.8	0.246	117.4
20	6	371.1	8.9	8.5	0.272	24.6
20	8	494.8	11.7	11.3	0.291	65.2
20	10	618.6	15.3	14.7	0.260	115.2
20	12	742.3	19.1	18.3	0.249	168.9

Figure 12 shows the variation of the average Nusselt number depending on the Reynolds number, which is defined according to the piezo fan tip velocity. The Nusselt number corresponding to the natural convection state in the case of no piezo fan placed in the channel was calculated as 6.80. The variation of the average Nusselt number on the channel surfaces with the Reynolds number is approximately linear, and a regression curve is proposed. It should be noted that four amplitudes are stated with different colors to highlight the effect of amplitude at the same Reynolds number. Results show that increasing the amplitude is more effective than increasing the frequency of the Nusselt number. The results can be used as a first approximation to evaluate the effect of amplitude and frequency while designing a thermal system, including a piezo fan.

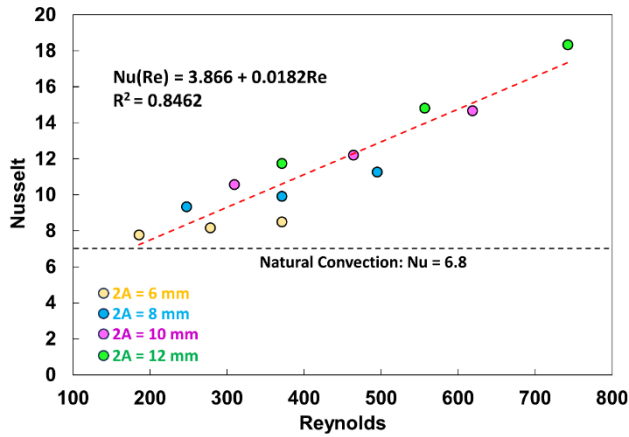


Figure 12. Variation of Nusselt number with Reynolds number

4. Conclusions

This study reveals the impacts of piezo fan's amplitude and frequency on the vortex structures and cooling performance. As a contribution to the literature, the current study highlights both the vortex structures, local and average heat transfer characteristics and proposes a Nusselt correlations in terms of the dimensionless Reynolds number defined regarding the tip speed of the blade. The following conclusions are evaluated:

- Increased amplitude and frequency facilitated greater air displacement and enhanced air mixing. The maximum increment in the flow rate is more than 180%.
- Increasing the amplitude at a lower frequency, i.e., 10 Hz, increases the outlet temperature. At higher frequencies, i.e., 20 Hz, a variation in the amplitude does not significantly alter the outlet temperature.
- The steady-state convection coefficient was calculated as 7.1 W/m²K for natural convection. With a frequency of 20 Hz and an amplitude of 12 mm, the enhancement in heat transfer coefficient is 169%.

As a further study, 3D analyses are suggested to comprehensively examine the effect of the piezoelectric fan motion on flow and heat transfer. Exploring diverse channel geometries with non-uniform thermal boundary conditions holds promise in advancing understanding, particularly in the context of electronic device applications.

Nomenclature

- A_{pz} : Piezo fan cross-sectional area (mm²)
 c_p : Specific heat (J/kgK)
 E_{pz} : Young's modulus (Pa)

- f : Frequency (Hz)
 g : Gravitational acceleration (m/s²)
 h : Heat transfer coefficient (W/m²K)
 \bar{h} : Average heat transfer coefficient (W/m²K)
 I : The second moment of area of piezo fan (m⁴)
 k : Thermal conductivity (W/mK)
 l_h : Length of the heated surface (mm)
 l_i : Length of the adiabatic surface (mm)
 l_{pz} : Length of the piezo fan (mm)
 \dot{m}' : The mass flow rate per unit depth (kg/ms)
 m_{pz} : Piezo fan mass (kg)
 Nu : Nusselt number ($\frac{\bar{h}w}{k}$)
 p : Pressure (Pa)
 Re : Reynolds number ($\frac{u_{tip}w}{\vartheta}$)
 t : Time (s)
 T : Temperature (K)
 u : x -component of the velocity (m/s)
 v : y -component of the velocity (m/s)
 q' : Heat transfer rate per unit depth (W/m)
 q'' : Heat flux (W/m²)
 w : Channel width (mm)
 x, y : Cartesian coordinates
 $x_{pz}(y, t)$: Instant amplitude of the piezo fan vertical orientation (m)
 $X_{pz}(y)$: Maximum piezo fan displacement at arbitrary y -location (m)

Subscripts

- init : Initial
o : Outlet
i : Inlet
a : Air
avg : Average
pz : Piezo fan
ref : Reference
h : Heated surface
disp : Displacement

Greek symbols

- β : Characteristic coefficient
 ψ : Dimensionless drive coefficient
 ϑ : Kinematic viscosity (m²/s)
 ρ : Density (kg/m³)
 Δ : Change or difference
 μ : Dynamic viscosity (Ns/m²)

Abbreviations

- ALE : Arbitrary Lagrangian-Eulerian
FSI : Fluid Structure Interaction
NC : Natural convection

References

- [1] Choi M, Lee SY, Kim YH. On the flow around a vibrating cantilever pair with different phase

- angles. *European Journal of Mechanics-B/Fluids*, 34, 146-157, 2012.
- [2] Liu SF, Huang RT, Sheu WJ, Wang CC. Heat transfer by a piezoelectric fan on a flat surface subject to the influence of horizontal/vertical arrangement. *International Journal of Heat and Mass Transfer*, 52(11-12), 2565-2570, 2009.
- [3] Wait SM, Basak S, Garimella SV, Raman A. Piezoelectric fans using higher flexural modes for electronics cooling applications. *IEEE Transactions on Components and Packaging Technologies*, 30(1), 119-128, 2007.
- [4] Lin CN. Analysis of three-dimensional heat and fluid flow induced by piezoelectric fan. *International Journal of Heat and Mass Transfer*, 55(11-12), 3043-3053, 2012.
- [5] Lin CN. Heat transfer enhancement analysis of a cylindrical surface by a piezoelectric fan. *Applied Thermal Engineering*, 50(1), 693-703, 2013.
- [6] Park SH, Oh MH, Kim YH, Choi M. Effects of freestream on piezoelectric fan performance. *Journal of Fluids and Structures*, 87, 302-318, 2019.
- [7] Tiwari J, Yeom T. Enhancement of channel-flow convection heat transfer using piezoelectric fans. *Applied Thermal Engineering*, 191, 116917, 2021.
- [8] Chen Y, Peng D, Liu Y. Heat transfer enhancement of turbulent channel flow using a piezoelectric fan. *International Journal of Heat and Mass Transfer*, 147, 118964, 2020.
- [9] Hasan SI, Küçüka S, Ezan MA. Thermo-fluidic analysis of a single piezo fan in longitudinal channel. *International Communications in Heat and Mass Transfer*, 129, 105651, 2021.
- [10] Hasan SI, Küçüka S, Ezan MA. Cooling performance of a piezo fan oscillating in a vertical channel with natural convection. *International Communications in Heat and Mass Transfer*, 141, 106602, 2023.
- [11] Sufian SF, Fairuz ZM, Zubair M, Abdullah MZ, Mohamed JJ. Thermal analysis of dual piezoelectric fans for cooling multi-LED packages. *Microelectronics Reliability*, 54(8), 1534-1543, 2014.
- [12] Sufian SF, Abdullah MZ. Heat transfer enhancement of LEDs with a combination of piezoelectric fans and a heat sink. *Microelectronics Reliability*, 68, 39-50, 2017.
- [13] Acikalin T, Garimella SV. Analysis and prediction of the thermal performance of piezoelectrically actuated fans. *Heat Transfer Engineering*, 30(6), 487-498, 2009.
- [14] Lei T, Jing-Zhou Z, Xiao-Ming T. Numerical investigation of convective heat transfer on a vertical surface due to resonating cantilever beam. *International Journal of Thermal Sciences*, 80, 93-107, 2014.
- [15] Wait SM, Basak S, Garimella SV, Raman A. Piezoelectric fans using higher flexural modes for electronics cooling applications. *IEEE Transactions on Components and Packaging Technologies*, 30(1), 2007.
- [16] Kimber M, Suzuki K, Kitsunai N, Seki K, Garimella SV. Pressure and flow rate performance of piezoelectric fans. *IEEE Transactions on Components and Packaging Technologies*, 32(4), 766-775, 2009.